



Analysis of compressible flow at the outlet of a convergent – divergent nozzle

Benaouda Douaiba*, Fadia Baghlad, Mohammed Hamel

Laboratory of Applied Mechanics, Faculty of Mechanical Engineering, University of Sciences and Technology of Oran, USTOMB El Mnaouar, BP 1505, Bir El Djir 31000, Oran, Algeria, email: dustmodeling@gmail.com (B. Douaiba)

Received 30 June 2022; Accepted 1 October 2022

ABSTRACT

In the present study, a numerical investigation of outflow regimes of a convergent-divergent nozzle was carried out. This analysis was based on a section ratio of nozzle area ration = 1.66 and on the influence of different expansion ratios nozzle pressure ration (NPR) on the downstream flow properties. Low and high expansions rates were examined, and two intervals were chosen, the first NPRL [1.27, 1.4], while the second was NPRH [5.5, 10]. The CFD technique was used to simulate 2D CD nozzle outflow of a supersonic jet engine. The NPRL results show the phenomenon of normal shock waves occurred when the back pressure was less than ambient pressure. However the NPRH results show Mach diamond patterns at the jet plume region. The obtained results were compared with experimental data.

Keywords: Nozzle; Compressible flow; STAR-CCM+; Expansion; Shock wave

1. Introduction

Studies around compressible flows [1], especially in convergent-divergent nozzles [2] have been the subject of several experimental and numerical investigations [3–5]. The supersonic convergent-divergent nozzle finds application in many areas of industry and technology. It plays a vital role in the aerospace industry, military and combat jets including rocket nozzles and missiles [6]. When the gas is expanded through a CD nozzle from subsonic to supersonic conditions, the flow undergoes several physical phenomena occurring internally such as shocks and flow separations as well as externally such as Mach shock diamonds and supersonic jets, that can influence the performance and reliability of the propulsion system [7–9]. These phenomena lead to pressure loss, thereby reduce the thrust generated by the nozzle. For example the loss in thrust due to Mach shock diamonds makes the nozzle less efficient [6,10]. The geometrical configuration of the nozzle designing the flow to minimise the thrust lost [11]. Numerous experimental and computational studies carried out by varying the nozzle area

ratio (NAR) have been performed in CD nozzles under nozzle pressure ratio (NPR) [3,6,12]. Most of their studies have been focused on the influence of the NPR on the flow properties downstream (divergent section) and the external (jet plume) region of the nozzle [5,7,13]. In the present work, the NAR is fixed to 1.66, for the symmetric nozzle. However the flow characteristics under low [1.27, 1.4] and high [5.5, 10] NPRs are tested numerically to investigate flow separations and shocks. As well as jet flow patterns at the plume regions and deflection properties.

2. Materials and methods

The CFD technique was employed to simulate the nozzle outflow. Under atmospheric conditions, a 2D symmetric CD nozzle of a supersonic jet engine (Fig. 1) was modeled and tested. The STAR-CCM+ code was used to solve Reynolds-averaged Navier-Stokes (RANS) equation with turbulence models. The governing equations, which include the conservation equations for mass, momentum, and energy, along with the equation of state were treated in generalized

* Corresponding author.

coordinates and in conservative form. The conservation of mass for compressible flow can be written as Eq. (1):

$$\frac{\partial}{\partial t} \oint_{\Omega} \rho d\Omega + \oint_{\Omega} \nabla \cdot (\rho V) d\Omega \quad (1)$$

where ρ is density and Ω is control volume. The divergence of the vector V is represented in the term $\nabla \cdot$. The fluid velocity is: $V = u_i + v_j$ where u, v are the velocity components in i and j directions.

Based on the Newton's second law, using divergence notation the integral form for momentum x direction [Eq. (2)]:

$$\oint_{\Omega} \frac{\partial(\rho u)}{\partial t} d\Omega - \oint_{\Omega} \nabla \cdot (\rho u V) d\Omega = \oint_{\Omega} \rho F_x d\Omega - \oint_{\Omega} \frac{\partial \rho}{\partial x} d\Omega \quad (2)$$

where p is pressure, F_x and F_y are additional surface forces, which are the shear and normal viscous stresses in x and y directions integrated over the control volumes.

Based on the first law of thermodynamics, Eq. (3) is given in integral form:

$$\begin{aligned} &\oint_{\Omega} \dot{q} \rho d\Omega - \oint_{\Omega} \nabla \cdot (pV) d\Omega + \oint_{\Omega} \rho (f \cdot V) d\Omega \\ &= \oint_{\Omega} \frac{\partial}{\partial t} \left[\rho \left(e + \frac{V^2}{2} \right) \right] d\Omega + \oint_{\Omega} \nabla \cdot \left[\rho \left(e + \frac{V^2}{2} \right) V \right] d\Omega \end{aligned} \quad (3)$$

where e is internal energy, and \dot{q} is the rate of heat added. $(e + V^2/2)$, this term represents the sum of internal and kinetic energies.

The expansion ratio (ratio of exit area to throat area) was $NAR = 1.66$. Low and high expansions rates were changed from NPRL [1.27, 1.4] to NPRH [5.5, 10]. A Trimmer mesh of two symmetric CD nozzle was conducted using STAR-CCM+ as shown in Fig. 2. The flow characteristics were specified by 21,517 elements and 10 as number of prism layer. However, the walls of the nozzle were considered adiabatic.

3. Results and discussion

3.1. Low NPRs: NPRL [1.27, 1.4]

Over-expansion occurred at low NPRs (Fig. 3a and b). The phenomenon of normal shock waves occurred when the back pressure was less than ambient pressure. These waves bent toward the jet plume. A mixed subsonic and supersonic flow at the exiting of the nozzle was formed when the shock wave was oblique to the wall. The flow reversal effected at the flow to detach from the surface. In this case a circulation bubble was created as well as a lambda foot shock at the triple point. Oblique shock waves were also encountered with the Mach disks (Fig. 3c).

3.2. High NPRs: NPRH [5.5, 10]

Further increasing NPR caused the back pressure to match the ambient pressure, resulting in a smooth flow, uniform supersonic and parallel. A new unsteadiness was created when the outlet pressure was greater than atmospheric pressure. However, an expansion wave occurred at the exit of the nozzle wall. For higher NPRs the results showed Mach diamond shock patterns at the jet plume region. While compression and expansion waves were repeated downstream along the plume region (Fig. 4).



Fig. 1. Geometry set-up with $NAR = 1.66$.

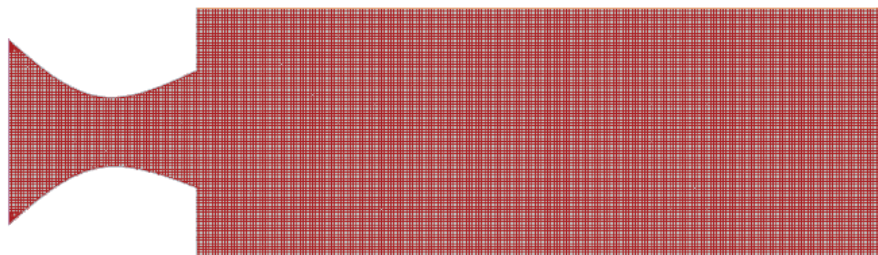


Fig. 2. Computational mesh set-up in STAR-CCM+.

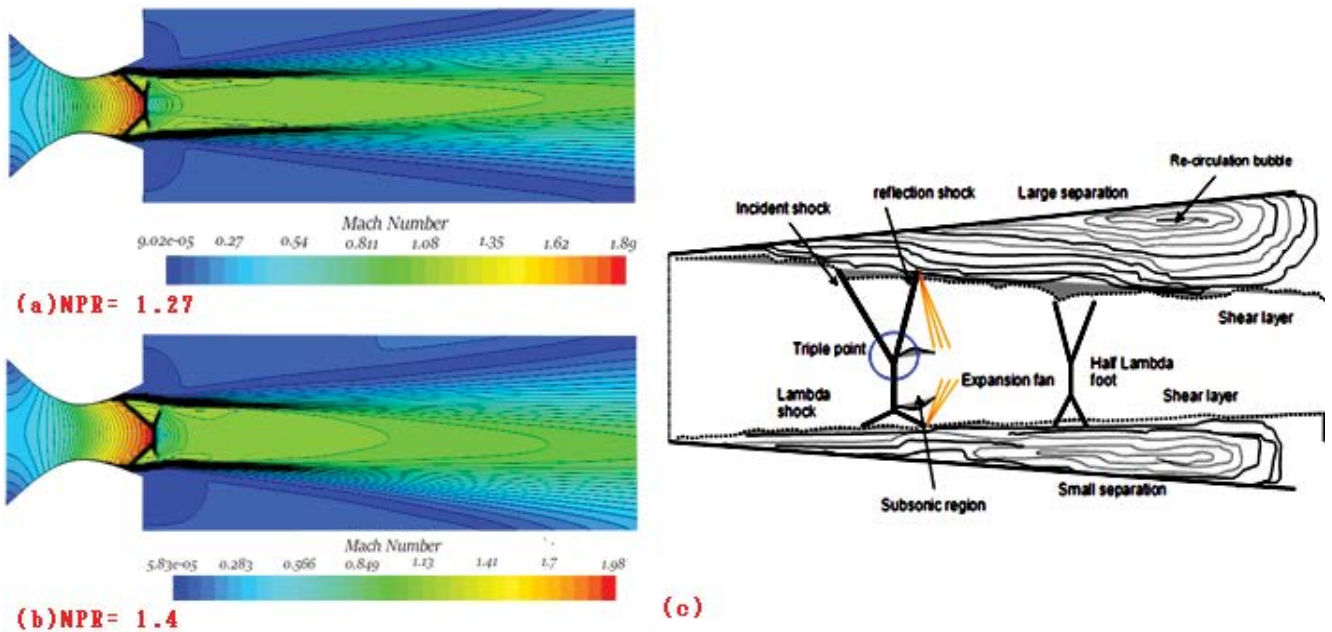


Fig. 3. Mach contours for low NPRs (a) 1.27, (b) 1.4, and (c) lambda foot shock wave and circulation bubble.

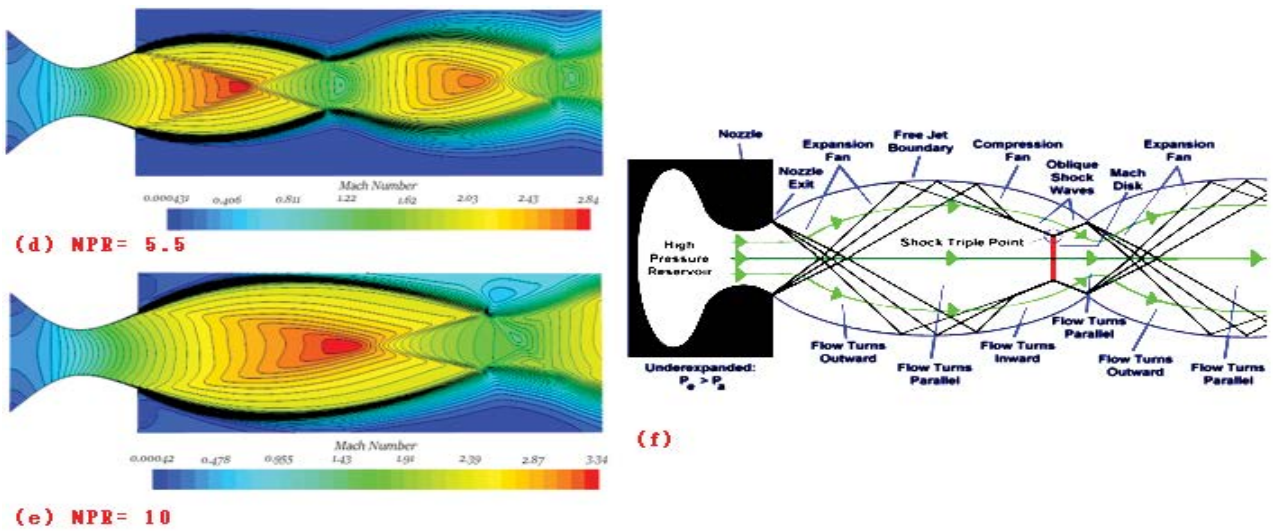


Fig. 4. Mach contours: maximum Mach number: (d) $M = 2.84$, (e) $M = 3.34$, outside the nozzle for high NPRs (d) 5.5, (e) 10 and (f) theoretical diagram of under-expansion flow.

3.3. Turbulent kinetic energy

The increasing static pressure contributed to increased potential energy of the gas thereby decreasing the kinetic energy of the flow (Fig. 5).

When the static pressure was increased (Fig. 6 for low NPRs), an adverse pressure gradient caused the boundary layer to separate from the nozzle wall surface.

4. Conclusions

The traditional CD symmetric nozzle model (NAR = 1.66) was examined under low and high NPRs, to

understand the internal flow phenomenon, lambda shocks and shock induced flow separation as well as the shock patterns (i.e., jet plume region) when the exiting internal flows at the end of the divergent section were immersed with the free stream flows at supersonic speeds. Once the back pressure was less than ambient pressure a normal shock wave was created. However, when an oblique shock was established at the divergent nozzle, a circulation bubble was created due to flow reversal. When the exit pressure at the divergent nozzle was greater than the ambient pressure, a Mach diamond shock was created and repeated downstream along a plum region. Consequently, the instability initiated by a shock wave at the divergent section

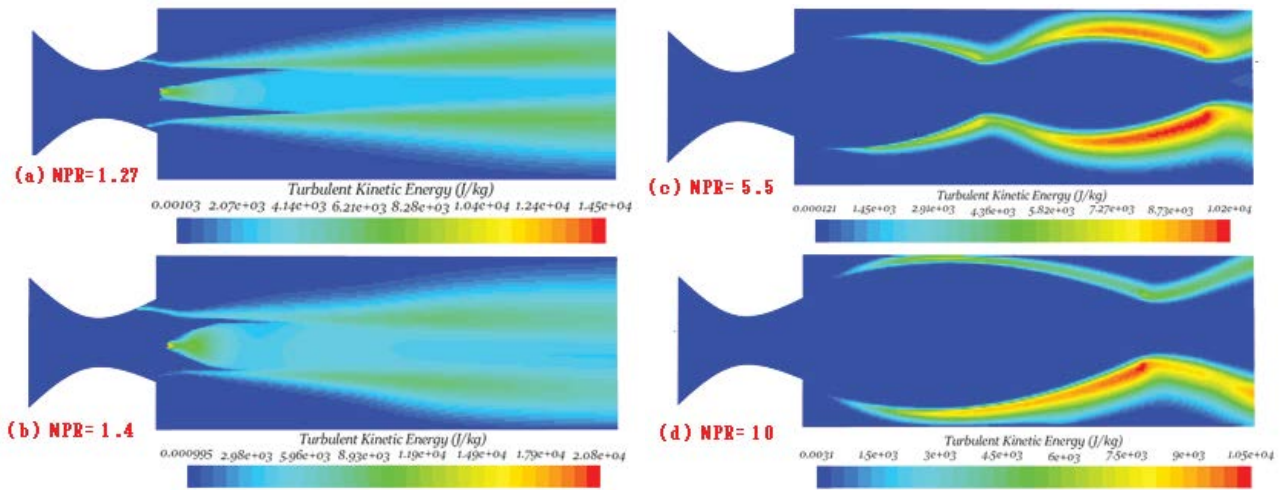


Fig. 5. Turbulent kinetic energy (TKE) values for NPR: (a) 1.27, (b) 1.4, (c) 5.5 and (d) 10.

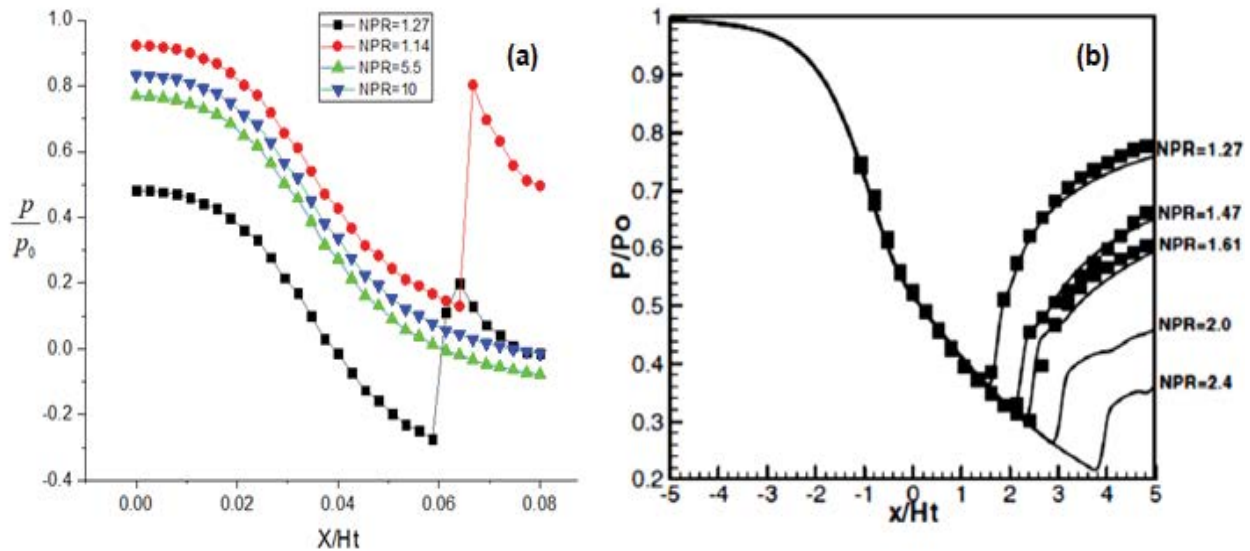


Fig. 6. (a) Numerical pressure distribution of NPRLS [1.27, 1.4, 5.5, 10] and (b) comparison of the pressure distribution on the wall of the divergent (the line indicates the calculation while symbol indicates experiments) Xiao et al. [12].

of a supersonic CD nozzle caused the exhaust gas to lose build-up fluid kinetic energy, hence decelerating the flow speed, and decreasing the overall thrust.

References

[1] S. Marimuthu, D. Chinnathambi, Computational analysis to enhance the compressible flow over an aerofoil surface, *Aircr. Eng. Aerosp. Technol.*, 93 (2021) 925–934.

[2] Z. Xia, Z. Xiao, Y. Shi, S. Chen, Mach number effect of compressible flow around a circular cylinder, *AIAA J.*, 54 (2009) 2004, doi: 10.2514/1.J054420.

[3] M. Harper-Bourne, The jet noise of a convergent-divergent nozzle, Session: Jet Aeroacoust. I: Exp. Jet Noise, (2022), doi: 10.2514/6.2022-2827.

[4] L. Zhou, Y.B. Meng, Z.X. Wang, Numerical study on flow characteristics of serpentine convergent-divergent nozzle, *Tuijin Jishu/J. Propuls. Technol.*, 42 (2021) 103–113.

[5] D. Modesti, S. Pirozzoli, F. Grasso, Direct numerical simulation of developed compressible flow in square ducts, *Int. J. Heat Fluid Flow*, 76 (2019) 130–140.

[6] Ekanayake, E.M. Sudharshani, Numerical Simulation of a Convergent Divergent Supersonic Nozzle Flow, Dissertation Submitted in Fulfilment of the Requirements for the Master of Science (Applied Mathematics), 2013.

[7] S.A. Khan, O.M. Ibrahim, A. Aabid, CFD analysis of compressible flows in a convergent-divergent nozzle, *Mater. Today: Proc.*, 46 (2021) 2835–2842.

[8] V. Zapryagaev, N. Kiselev, D. Gubanov, Shock-wave structure of supersonic jet flows, *Aerospace*, 5 (2018) 60, doi: 10.3390/aerospace5020060.

[9] I. Sadreghighi, Case Studies Involving Numerical Shock Wave/Boundary Layer Interactions (SWBLI), Independent CFD Researcher, 2022, doi: 10.13140/RG.2.2.26155.92961.

[10] A. Nebbache, Separated Nozzle Flow, CR MECANIQUE, 2018.

[11] B. Simon, Design and Optimization of Aircraft Engine Nozzles in Under-Wing Configuration, General Mathematics, HAL Open Science, 2020.

[12] Q. Xiao, H.M. Tsai, D. Papamoschou, A. Johnson, Experimental and numerical study of jet mixing from a shock-containing nozzle, *J. Propul. Power*, 25 (2009) 688, doi: 10.2514/1.37022.